Romanian Reports in Physics, Vol. 62, No. 4, P. 897–905, 2010

NEW APPROACH ON THE EXCITATION AND DAMPING OF TRANSVERSAL CORONAL LOOP OSCILLATIONS

G. MOCANU, A. MARCU

[1] *"Babeş Bolyai" University, Mihail Kogalniceanu Street nr. 1,*

400084 Cluj Napoca, Romania, E-mail:gabimocanu_ro@yahoo.com Email: amarc@phys.ubbcluj.ro

(Received November 13, 2009)

Abstract. The imaging telescope on board the Transition Region And Coronal Explorer (TRACE) spacecraft offered observations with high spatial resolution and unprecedented time cadence about spatial oscillations of solar coronal loops. Current theoretical models attempt to explain the excitation mechanism, rapid damping and selectivity of these oscillations. The theoretical model presented here simulates the interaction between magnetic flux tubes and a shock wave generated by an explosive flare event. As a key feature of the model, the subsequent observed damping is considered to occur due to the opposition of the external magnetized medium to the perpendicular propagation of a medium/low velocity disturbance. Comparison of the theoretical damping results of the model with observational data gives an excellent agreement.

Key words: transversal oscillation, damping, shock wave.

1. INTRODUCTION

Observations supplied by TRACE in the 171Å filter show spatial displacement of solar coronal loops [1, 2, 10, 17]. They are dubbed "transversal mode", as it is observed that plasma inside the loop moves as a whole, perpendicular to the equilibrium magnetic field. These oscillations are considered to be triggered by massive releases of energy nearby, such as flares, CMEs or filament destabilization. Based even on visual inspection only (full movies of the events are available at http://vestige.lmsal.com/TRACE/POD/TRACE oscillations.html, courtesy of [16]), it is clear that the loops' footpoints are not displaced and that the oscillation damps on time scales comparable to the loops' oscillation periods. Another puzzling observational fact is that only a small percent of the flares are accompanied by oscillating loops [2].

The theoretical models must supply valid explanations for the values of the oscillation periods and damping times and must also explain the excitation

mechanism and why not all loops oscillate (selectivity of excitation). Types of models proposed to explain excitation mechanism, damping mechanism or both are: damping due to footpoint leakage of Alfven waves [4], damping due to phase mixing [13], viscous damping with anomalous low Reynolds number [9], viscous damping due to small viscosity scales [11], destabilization of magnetic sources in the photosphere and damping due to subsequent relaxation of magnetic field lines [17], excitation and damping due to dispersive nature of the magnetized medium inside and outside the loop [18], damping due to resonant absorption [15], excitation due to vortex shedding [7]. The common aspects of these models are the association of a flare event with transversal oscillations of coronal loops and the identification of the oscillation mode as the fast kink mode of a magnetic flux tube.

One of the basic ideas of this article is that the excitation mechanism can be attributed to a shock wave traveling towards the loop as the result of a flare nearby. The chosen geometry requires that the wave travels perpendicular to the exterior magnetic field, thus the shock wave is considered to be a fast magnetoacoustic shock and the impact point is the loop apex. Following the impact, the loop begins to oscillate and the reported maximum velocity is of the order of 10 km/s [2, 16]. Another important idea is that the damping of the induced oscillation occurs as a result of the opposition of the external magnetic field to a transversal slowly propagating oscillation. The analytical treatment is carried without using mathematical constraints such as the fact that the mode might be a kink mode. The solution must only satisfy the observed boundary condition of fixed footpoints.

In Section 2 the mathematical treatment is developed, while in Section 3 the results are presented and discussed. Conclusions follow in Section 4.

2. MATHEMATICAL APPROACH

The configuration under analysis consists of a magnetic flux tube approximating the line tied coronal loop. In a coordinate system fixed with the loop, the flux tube is aligned with its equilibrium magnetic field $\vec{B}_0$ and the z axis. The internal and external magnetic fields are of the same order of magnitude and if they are not parallel, they are at least coplanar in the yOz plane. The shock wave, moving parallel to the x axis, hits the loop in the apex exerting a force $\vec{F}_{sh}$. The response of the external medium to the oscillations of the loop is given by a force $\vec{F} = \alpha\vec{v}$, where α is a constant and $\vec{v}$ is the velocity of the incoming loop.

The linearized magnetohydrodynamic equations, in the $\beta \to 0$, approximation are:

$$\begin{aligned}
&\frac{\partial \rho}{\partial t} + \nabla \cdot (\rho_0 \vec{v}) = 0, \\
&\rho_0 \frac{\partial \vec{v}}{\partial t} = \frac{1}{\mu_0}\left(\nabla \times \vec{B}\right) \times \vec{B}_0 + \rho \vec{g} + \vec{F}_{sh} + \alpha \vec{v}, \\
&\frac{\partial p}{\partial t} - c_S^2 \frac{\partial \rho}{\partial t} - \rho_0 g v_z = 0, \\
&\frac{\partial \vec{B}}{\partial t} = \nabla \times \left(\vec{v} \times \vec{B}_0\right), \\
&\nabla \cdot \vec{B} = 0,
\end{aligned} \tag{1}$$

where $\beta = \frac{2\mu_0 p}{B_0^2}$ is the plasma beta coefficient, c_S is the sound speed inside the loop, ρ_0 is the equilibrium density of the internal medium, g is the gravitational acceleration at the solar surface and $p, \rho, \vec{v}, \vec{B}$ represent the perturbations of the pressure, density, velocity and magnetic field around their equilibrium values.

Solving this system for $v_x = \vec{v} \cdot \hat{x}$, the governing equation for transversal velocity of the loop displacement is derived as:

$$\frac{\partial^2 v_x}{\partial t^2} - v_A^2 \frac{\partial^2 v_x}{\partial z^2} = \frac{1}{\rho_0} \frac{\partial F_{sh}}{\partial t} + \frac{\alpha}{\rho_0} \frac{\partial v_x}{\partial t}, \tag{2}$$

where $v_A^2 = B_0^2 / (\rho_0 \mu_0)$ is the Alfven speed characterizing the plasma inside the loop.

This equation can be Fourier analyzed in time by writing $v_x(z) = \tilde{v}_x(z) \exp(i\omega t)$, with:

$$\omega = \omega_R + i\omega_I . \tag{3}$$

This allows for the mathematical representation of the damping through the presence of a nonzero ω_I, while the real part of the frequency, ω_R, gives the period of oscillation. Substitution of (3) into (2) leads to two equations, one for a real part and another for an imaginary part. The equation for the imaginary part can be used to find α:

$$\alpha = \frac{1}{\tilde{v}_x} \frac{\partial F_{sh}}{\partial t} e^{\omega_I t} \frac{\sin\left(\omega_R t\right)}{\omega_R} - 2\rho_0 \omega_I . \tag{4}$$

After replacing (4) back into the real part of (2), the equation for the amplitude of transversal velocity becomes:

$$\left(\omega_R^2+\omega_I^2\right)\tilde{v}_x+v_A^2\frac{\mathrm{d}^2\tilde{v}_x}{\mathrm{d}z^2}=\frac{1}{\rho_0}\frac{\partial F}{\partial t}\mathrm{e}^{\omega_I t}\left[\frac{\omega_I}{\omega_R}\sin\left(\omega_R t\right)-\cos\left(\omega_R t\right)\right]. \tag{5}$$

The analytical form of $\vec{F}_{sh}$ must account for a short temporal interaction and a localized spatial impact. This is done by using a Heaviside step function for the time dependence and a Gaussian centered on the point of impact for the space dependence:

$$\begin{aligned}&\vec{F}_{sh}(z,t)=F(x,t)\hat{x},\\&F(z,t)=F_0H(\tau-t)\frac{1}{a\sqrt{\pi}}\left[\mathrm{e}^{-(z-z_0)^2/a^2}+\mathrm{e}^{-(z-L+z_0)^2/a^2}\right],\end{aligned} \tag{6}$$

where the numerical value of F_0 is given by the assumption that the incoming wave is a fast MHD shock, τ is the temporal duration of the interaction and a is the width of the spatial shock.

3. RESULTS AND DISCUSSION

The solution of eq. (5) and observational data [1, 2, 3, 9, 16] were used to create columns 7–11 in Table 1, where c is the percent from the energy of the incoming wave fitted to obtain observed displacement amplitudes and damping times. Numerical values from columns 7 and 8 were fitted for a fixed density contrast ($\rho_{\mathrm{ext}}/\rho_{\mathrm{int}}=0.1$) while columns 10 and 11 were obtained when observational data regarding density contrast, n, was also available (see column 9).

Table 1

The observational and computed data for 12 loops

	L[Mm]	P[s]	t_d[s]	A[Mm]	v_A[km/s]	ω_I[Hz]10^{-3}	c[%]	n	ω_I^*[Hz]10^{-3}	c^*[%]
1[a]	168	261	1200	0.8	2600	-0.7944	1.7	0.2	-0.7944	1.71
2[b]	72	265	300	2	2600	-4-7420	19	0.26	-4.3863	19
3[c]	174	316	500	6	2600	-2.7240	18	0.27	-2.7240	18
4[d]	204	277	400	4	2500	-3.3570	8.7	0.42	-3.3570	8.7
5[e]	162	272	849	5	3000	-1.0279	12.5	0.44	-1.0233	12.5
6[f]	258	435	600	0.7	2500	-1.5888	1.25	0.14	-1.5888	1.25
7[g]	146	396	400	1.8	3500	-4.7600	12.5	0.66	-5.0773	13
8[h]	258	435	600	-	839	-1.0833	4.5	-	-	-
9[i]	166	143	200	-	1640	-3.5150	8	-	-	-

Table 1 (continued)

10[j]	406	423	800	-	1360	-0.8912	3	-	-	-
11[k]	192	185	200	-	1470	-4.5850	7	-	-	-
12[l]	340	630	1000	4	2000	-1.3464	5.5	-	-	-

1[a] previously described in [2, 16], triggered by a M4.6 flare, event on 14 Jul 1998, 12:45 UT, their loop 1a.
2[b] (idem 1[a]), their loop 1b.
3[c] (idem 1[a]), their loop 1d.
4[d] (idem 1[a]), their loop 1f.
5[e] (idem 1[a]), their loop 1g.
6[f] previously described by [2, 16], triggered by a C4.6 flare, event on 4 July 1999, 08:33 UT, their loop 4a.
7[g] previously described by [2, 16], triggered by a C3.8 flare, event on 15 June 2001, 06:35 UT, their loop 17a.
8[h] previously described by [12], 4 July 1999, ω_I and c calculated for A=1.7Mm, their loop 7.
9[i] previously described by [12], event on 25 Oct. 1999, ω_I and c calculated for A=1.9Mm, their loop 8.
10[j] previously described by [12], event on 21 March 2001, ω_I and c calculated for A=1.8Mm, their loop 9.
11[k] previously described by [12], event on 15 May 2001, ω_I and c calculated for A=1.9Mm, their loop 10.
12[l] previously described by [20], event on 27 June 2007, triggered by a C1.3 flare.

From the number of oscillations discussed in the literature, the events presented in Table 1 were chosen on certain criteria: the flare had to be near the loop, but not localized at one of its footpoints or underneath it; also, other reported oscillations where uncertainties in observational data were large were not considered.

The RHS of (5) contains an exponential with a real time dependent exponent, acting as an envelope of the temporal evolution of the velocity. This appears naturally in the model and, as seen in Table 1, its value is within the same order of magnitude for all the loops discussed, except for loops 1 and 10 (this enters in the area of observational error). For the cases when a displacement amplitude was available from observational data (loops 1–7 and 12), the energy needed to induce the observed oscillations is calculated to represent 1%–10% from the energy of a fast MHD mode hitting the loop.

By comparison of columns 10 and 11 with 7 and 8, another fact, sustained by previous observations, becomes apparent: the damping coefficient ω_I, and energy conversion percentage c, are not sensitive to changes in density contrast; this holds for accepted coronal values of $\rho_{ext}/\rho_{int} < 1$. For every loop, a graph was plotted representing the displacement of the loop apex as a function of time. The agreement with observational data from [2] and [16] is very good. Presented here are only two examples: loops 1 (Fig. 2) and 6 (Fig. 4), with the observational plots also shown for comparison purpose (Fig. 1 and Fig. 3).

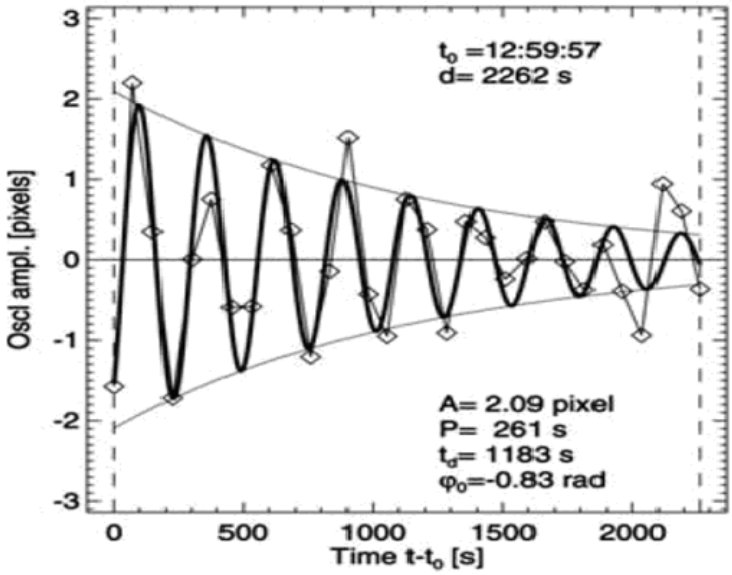

Fig. 1 – Observational evolution of loop 1 (courtesy of [2, 16]).

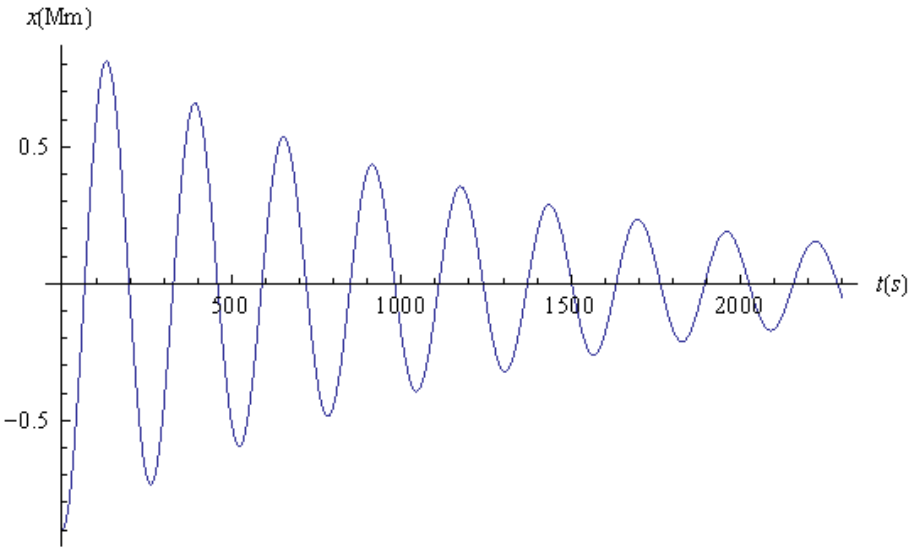

Fig. 2 – Evolution of loop 1 according to our model.

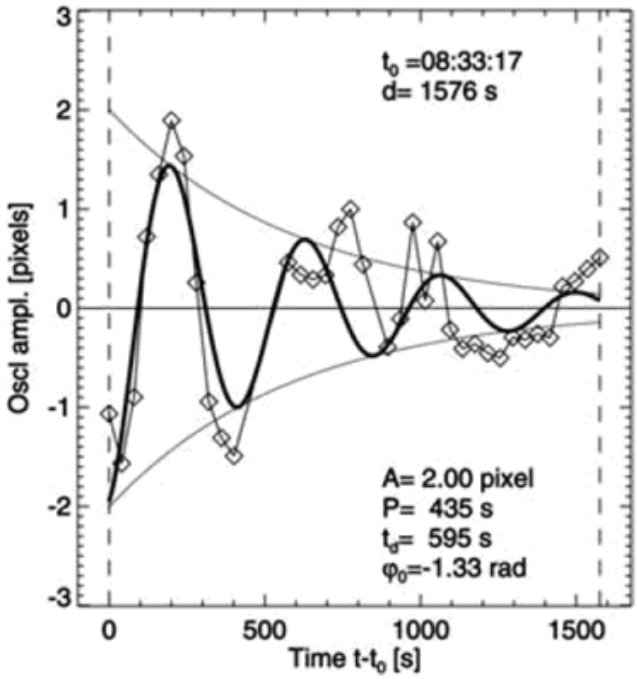

Fig. 3 – Observational evolution of loop 6 (courtesy of [2, 16]).

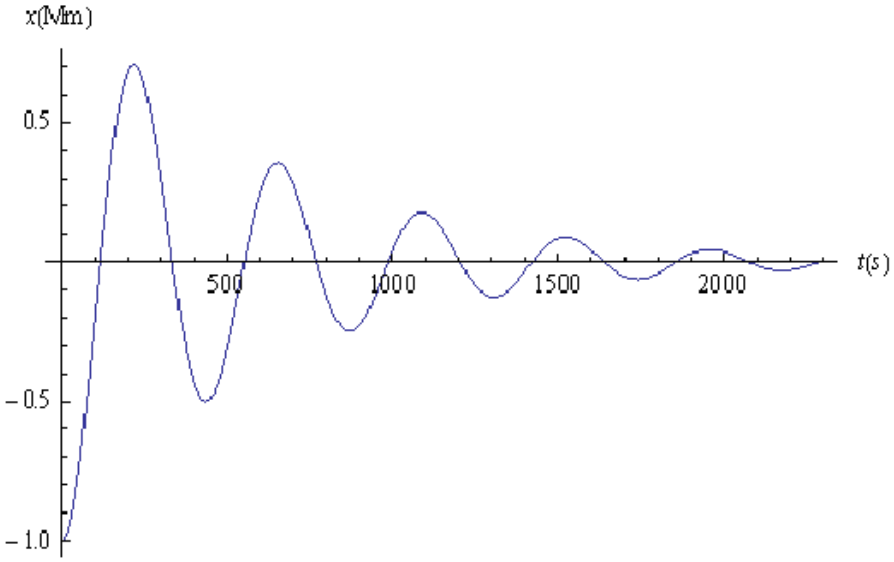

Fig. 4 – Evolution of loop 6 according to our model.

The numerical values of the ordinate do not correspond because the observational graph is scaled in pixels, but the maximum displacement is converted in Mm in column 5 of Table 1.

4. CONCLUSIONS

This study is an analytical approach to the issue of excitation and damping of transversal coronal loop oscillations. By using observational data it was shown that the model describes to a high degree of accuracy the observed behavior of coronal loops following impact with a shock wave.

The two key points of the model are the analytical shape of the driving force (eq. (6)) and the inclusion of a force to account for the opposition of the external magnetized medium to low velocity transversal disturbances (equation of motion from eq. (1)). Values obtained for the ω_I coefficient of the decaying time exponential are within the same order of magnitude for all the analyzed loops, as seen in Table 1, column 7. Also, the percentage of the energy of the incoming shock wave needed to produce the observed oscillations presents a low numerical dispersion (Table 1, column 8) and neither ω_I nor c is sensitive to changes in the density contrast (Table 1, columns 10 and 11). These facts lead to the conclusion that our initial assumption was correct; namely, the damping of transversal oscillations is a global characteristic of the solar corona and not something particular to one loop.

There is one important issue still to be addressed and future work will focus on that. In this stage, the model does explain the selectivity of excitation as it is observed. We suggest that this could be obtained by modeling the more realistic case when α is not constant, but depends directly on the magnetic properties of the external medium.

Aknowledgements. The authors aknowledge the financial support by the Romanian National University Research Council (CNCSIS-PN-II/531/2007).

REFERENCES

1. M. J. Aschwanden, L. Fletcher, C. J. Schrijver, D. Alexander, Ap. J., **520**, 880–894 (1999).
2. M. J. Aschwanden, B. De Pontieu, C. J. Schrijver, A. M. Title, So. Phys., **206**, 99–132 (2002).
3. M. J. Aschwanden, R. W. Nightingale, J. Andries, M. Goossens, T. Van Doorsselaere, Ap. J., **598**, 1375–1386 (2003).
4. B. De Pontieu, P. C. H. Martens, H. S. Hudson, Ap. J., **558**, 859–871 (2001).
5. M. Goossens, J. Andries, M. J. Aschwanden, Astron. Astrophys., **394**, L39–L42 (2002).
6. V. M. Nakariakov, Science, **12**, 1804–1813 (2007).

7. V. M. Nakariakov, M. J. Aschwanden, T. Van Doorsselaere, Astron. Astrophys., **502**, 661–664 (2009).
8. V. M. Nakariakov, L. Ofman, Astron. Astrophys., **372**, L53–L56 (2001).
9. V. M. Nakariakov, L. Ofman, E. E. DeLuca, B. Roberts, J. M. Davila, Science, **285**, 862–864 (1999).
10. L. Ofman, Ap. J., **568**, L135–L138 (2002).
11. L. Ofman, Adv. Space Res., **36**, 1572 (2005).
12. L. Ofman, M. J. Aschwanden, Ap. J., **576**, L153–L16 (2002).
13. B. Roberts, So. Phys., **193**, 139–152 (2000).
14. M. S. Ruderman, R. Erdelyi, Space Sci. Rev. published online, 2009.
15. M. S. Ruderman, B. Roberts, Ap. J., **577**, 475–486 (2002).
16. C. J. Schrijver, M. J. Aschwanden, A. M. Title, So. Phys., **206**, 69–98 (2002).
17. C. J. Schrijver, D. S. Brown, Ap. J., **537**, L69–L72 (2000).
18. J. Terradas, R. Oliver, J. L. Ballester, Ap. J., **618**, L149–L152 (2005).
19. Y. Uchida, So. Phys., **4**, 30–44 (1968).
20. E. Verwichte, M. J. Aschwanden, T. Van Doorsselaere, C. Foullon, V. M. Nakariakov, Ap. J., **698**, 397–404 (2009).
21. E. Verwichte, V. M. Nakariakov, L. Ofman, E. E. DeLuca, ESASP, **575**, 460–464 (2004).